ISSN 0915-633X

NATIONAL INSTITUTE FOR FUSION SCIENCE

Launching Conditions for Electron Cyclotron Heating in a Sheared Magnetic Field

K. Nagasaki, A. Ejiri

(Received - Dec. 14, 1994)

NIFS-330 Jan. 1995

RESEARCH REPORT
NIFS Series

NAGOYA, JAPAN

Launching Conditions for Electron Cyclotron Heating in a Sheared Magnetic Field

K. Nagasaki
Plasma Physics Laboratory
Kyoto University
Uji, Kyoto 611, Japan

A. Ejiri
National Institute for Fusion Science
Furoh-cho, Chikusa-ku, Nagoya 464-01, Japan

Abstract

Launching conditions for an electron cyclotron wave in a plasma with a sheared magnetic field are studied. One dimensional second order coupled equations are solved for the ordinary and extraordinary modes. It is shown that for wave absorption, the rotation angle and ellipticity of the wave should be determined by taking into account the effect of the sheared magnetic field, particularly in heliotron/torsatron configurations. Launching conditions for effective heating are obtained for second harmonic extraordinary-mode heating in the Heliotron-E, CHS and LHD helical devices.

Keywords: ECH, heliotron/torsatron, magnetic shear, launching condition

Electron cyclotron heating (ECH) is an advantageous heating tool for fusion plasmas. It is known that electron cyclotron waves have good coupling with a plasma. Optimally, the launched ECH power should be absorbed in a single pass in order to make the power deposition profile narrow. In helical systems, the fundamental and second harmonic ECH have been successfully applied to produce and heat a currentless plasma [1]. Usually the launching conditions for ECH were determined only by the direction of the resonant magnetic field. For example, for the extraordinary(X)-mode heating, the wave is launched so that the electric field is perpendicular to the orientation of the magnetic field at the resonance position. However, in heliotron/torsatron configurations like Heliotron-E, CHS and ATF, we have moderate or large magnetic shear, particularly, at the plasma boundary. Since the launched wave is coupled to the plasma at the boundary, the orientation of the magnetic field at the boundary is an important factor. Furthermore, the space-dependent magnetic field could affect the wave propagation. Our main concern is to study the propagation of the electron cyclotron wave in a plasma with a sheared magnetic field and to obtain the launching conditions for effective heating.

Shear effects on the wave propagation have been studied from the viewpoint of electron cyclotron emission (ECE) diagnostics [2]-[5] and polarimetric measurements [6]. Bell et al. investigated the polarization rotation of the electron cyclotron radiation with the third harmonic X-mode on ATF, and experimentally and theoretically showed that the wave did not emerge with the same polarization it had at its source. The polarization of the wave leaving the plasma is changed by the magnetic shear.

In this letter, we apply the calculation method used for plasma diagnostics, in order to investigate how the launched wave can access the resonance region. The propagation of the launched wave for electron cyclotron heating is studied in a sheared magnetic field, especially, in the Heliotron-E helical

device [7]. Recently a new ECH system has been installed in Heliotron-E [8], and the plasma experiment has been performed with 106.4GHz second harmonic ECH [9]. Launching conditions of ECH power at this frequency are calculated for effective heating.

Fixed Cartesian co-ordinates are used in this letter. The microwave propagates in the z-direction which is along the density gradient and perpendicular to the magnetic field. The magnetic field $\mathbf{B}$ is sheared in the $x-y$ plane. We define θ as the angle that the magnetic field makes with the x axis, $\theta = \tan^{-1}(B_y/B_x)$. Since B_z is negligibly small in Heliotron-E ($\mid B_z/B \mid \lesssim 3 \times 10^{-5}$), this simple slab model is applicable. Thermal and relativistic effects on the polarization are neglected in order to clarify the shear effect. The second order coupled equations for the ordinary(O)- and X-modes are given as [2]

$$\frac{d^2\hat{E}_{\parallel}}{dz^2} + (\frac{\omega^2}{c^2}N_O^2 - \phi^2)\hat{E}_{\parallel} = 2\phi\frac{d\hat{E}_{\perp}}{dz} + \frac{d\phi}{dz}\hat{E}_{\perp} \tag{1}$$

$$\frac{d^2\hat{E}_{\perp}}{dz^2} + (\frac{\omega^2}{c^2}N_X^2 - \phi^2)\hat{E}_{\perp} = -2\phi\frac{d\hat{E}_{\parallel}}{dz} - \frac{d\phi}{dz}\hat{E}_{\parallel} \tag{2}$$

where $\hat{E}_{\parallel} = \hat{E}_x\cos\theta + \hat{E}_y\sin\theta$, $\hat{E}_{\perp} = -\hat{E}_x\sin\theta + \hat{E}_y\cos\theta$, $N_O^2 = 1-p$, $N_X^2 = \{(1-p)^2-q\}/(1-p-q)$, $p = \omega_p^2/\omega^2$, $q = \omega_c^2/\omega^2$. N_O and N_X are the refractive indices for the O- and X-modes in a cold plasma, respectively. ω_p, ω_c and ω are the plasma frequency, cyclotron frequency and frequency of the launched microwave, respectively. Here, the shear $\phi = d\theta/dz$ is defined to be the angular gradient of the magnetic field in the z direction. $\hat{E}_{\parallel}$ and $\hat{E}_{\perp}$ refer to the components parallel and perpendicular to the local magnetic field direction, respectively. They are normalized by the initial total intensity. The initial launching condition are illustrated in Fig.1. γ is the ellipticity

defined as $\gamma = \tan^{-1}(b/a)$, β is the rotation angle that the long axis of the ellipse makes with the x-axis, where a and b are short and long radii of the ellipse, respectively. The condition $\gamma = 0$ corresponds to linear polarization. The electric field can be numerically calculated by integrating eqns. (1) and (2) along the propagation path. We consider the second harmonic X-mode heating in this letter. The effect of the electron cyclotron absorption is included in the numerical calculation. The second harmonic X-mode is strongly damped at the resonant layer, while the second harmonic O-mode and higher modes are weakly damped [6][10]. The absorption coefficient at the perpendicular injection to a Maxwellian distribution of velocities is derived from the Kirchhoff's law in the following form

$$\alpha^{(O,X)}(\omega) = (\frac{\omega_p^2}{\omega_c c}) \sum_{n \geq \nu} \sqrt{2\pi} \frac{\mu^{\frac{5}{2}}}{\nu^4} n^2 \sqrt{n^2 - \nu^2} \exp\{-\mu(\frac{n}{\nu} - 1)\} \frac{(n^2 - \nu^2)^n}{(2n+1)!} A_n^{(O,X)} \tag{3}$$

where $\nu = \omega/\omega_c$ and $\mu = m_e c^2/T_e$. For nonrelativistic energies ($T_e \lesssim 1keV$), A_n is given by

$$A_n^{(O,X)} = \Big(\frac{1 - (\frac{\nu}{n})^2}{2n+3}; 1\Big). \tag{4}$$

The optical depth is given as $\tau \equiv \int \alpha(\omega) ds$, where s is the distance along the propagation path. From eqn.(3), we find that the absorption is shifted in frequency, that is, $\alpha(\omega)$ has maximum at a slightly lower frequency than $n\omega_c$, and the absorption spectrum is broadened by the broadning of the energy distribution.

In the absent of plasma ($n_e = 0$), eqns.(1)(2) are reduced in the following form.

$$\frac{d^2\hat{E}_x}{dz^2} + \frac{\omega^2}{c^2}N^2\hat{E}_x = 0 \tag{5}$$

$$\frac{d^2\hat{E}_y}{dz^2} + \frac{\omega^2}{c^2}N^2\hat{E}_y = 0 \tag{6}$$

where $N^2 = N_O^2 = N_X^2 = 1$. $\hat{E}_x$ and $\hat{E}_y$ are kept constant, that is, the orientation of the electric field is independent of the background magnetic field. The same situation also occurs at $N_O^2 = N_X^2$.

Figure 2 shows the electric field along the z-axis for the Heliotron-E configuration. Since the electric field oscillates with a period $\lambda = 2\pi c/N\omega$, the envelope of the oscillation is plotted. The launched wave frequency is 106.4GHz, which corresponds to the second harmonic resonant mode at $B = 1.9T$. The electron density profile is assumed to be broad, $n_e(z) = n_e(0)\{1-(z/a)^6\}, n_e(0) = 1\times 10^{19}m^{-3}$, and the electron temperature profile is assumed to be parabolic, $T_e(z) = T_e(0)\{1-(z/a)^2\}, T_e(0) = 1keV$, which have been observed in typical ECH plasmas on Heliotron-E [11]. The wave is launched from the top of the torus, $z = 0.4m$. The plasma boundary is set to $0.3m$, which corresponds to the minor radius of the last closed magnetic surface of Heliotron-E. Initially, the launched wave is linearly polarized, $\hat{E}_x = 1, \hat{E}_y = 0$ ($\gamma = 0°, \beta = 0°$), that is, E is perpendicular to the axial magnetic field $B(0)$. Since we are interested in a plasma below the cut-off density, the backward propagating wave does not come into existence unless the reflection at the wall is considered. Therefore we treat only the forward propagating wave. If we launch the wave perpendicular to the magnetic field on axis, then 70% of the power is absorbed, and the remaining power escapes from the plasma in the single path. In Heliotron-E, when the resonance layer is located at the high field side (the helical coil side), that is, $B(0) < 1.90T$, then the wave does not cross the resonance layer, resulting that the power is

weakly absorbed. In such a case, we can see that the envelope of the electric field oscillates along the propagation path, which means that both the X- and O-mode do not propagate independently.

For effective heating and localization of the absorbed ECH power, it is desirable to optimize the launching conditions. Figure 3 shows dependence of the absorbed power on the launching conditions. The absorbed power P_{abs} is defined by $P_{abs} = 1 - N_O(-a)\hat{E}_{\parallel}(-a)^2 - N_X(-a)\hat{E}_{\perp}(-a)^2$, respectively. Here $-a$ corresponds to the boundary position of the opposite side. The plasma profile is the same as in Fig.2. At $\gamma = 15°, \beta = -30°$ and right rotation, the launched wave is converted into almost the pure X-mode, and the absorbed power becomes nearly 100% in the single path. The power deposition profile could be peaked. The rotation parameter $\beta = -30°$ means that the the launched wave is absorbed better when the electric field is close to be perpendicular to the magnetic field at the plasma boundary. At $\gamma = 45°$, the absorbed power does not depend on the rotation angle β, because the wave is circularly polarized.

In Fig.4 the $n_e(0)$ dependence of the absorbed power is shown. The density profile is fixed to be broad as given in Fig.2. The oscillation period of the envelope seen in Fig.2 becomes shorter with the increase of the density. This density dependence is due to the different density dependencies of refractive indices for the O- and X-mode. When the density is very low, $n_e(0) \lesssim 0.3 \times 10^{19} m^{-3}$, P_{abs} is small due to a weak absorption. We find that P_{abs} is larger than 95% of the total power, from $n_e(0) \simeq 1 \times 10^{19} m^{-3}$ to near the cut-off density, $7 \times 10^{19} m^{-3}$, when we choose the launching conditions as $\gamma = 15°, \beta = -30°$ and right rotation. This feature is convenient, as it is difficult to modify the polarization according to variation in density during the plasma discharge.

The plasma boundary position should also be considered. From several probe measurements, it was experimentally observed that there was a

scrape-off layer(SOL) plasma outside the LCFS, but the density decreased exponentially around the LCFS [12]. When the plasma boundary position used in the calculation is changed from $a = 0.3$ to 0.33, corresponding to the ambiguity in the experimentally measured position, the change in P_{abs} was less than 10%.

These calculations are applicable to other helical devices. Calculation results show that for second harmonic heating with the wave launched perpendicular to B, P_{abs} is 78% in CHS($53.2GHz$) and 77% in LHD ($84GHz$). Though the rotational transform of these devices are smaller than that of Heliotron-E, the magnetic shear θ at the edge is high, $\theta \sim 40°$, giving rise to low efficiency. Optimization of the launching conditions are listed in Table I. The rotation angle has an opposite sign between Heliotron-E and CHS, because the helical coil has a right-handed winding in the counterclockwise direction viewed from the top in Heliotron-E and has a left-handed one in CHS.

In summary, the propagation of the electron cyclotron wave for ECH was studied in a plasma with a sheared magnetic field, in particular, in heliotron/torsatron configurations. The wave propagation and the absorbed power ratio were calculated by solving the second order coupled equations. It was shown that the magnetic shear effects should be taken into account for effective ECH. The launching conditions for the second harmonic X-mode ECH were calculated on Heliotron-E, CHS and LHD.

The rotation angle and ellipticity can be easily controlled by a polarizer [13] [14]. Such a polarizer is planned to be installed in the 106.4GHz ECH system of Heliotron-E. Using this polarizer, the shear effect will be experi-

mentally studied in the near future.

Acknowledgement

One of Authors (K.N.) thank the Heliotron-E staff for continuous discussions. He also thanks Dr. B. J. Peterson for useful discussions. Encouragement by Profs. T. Obiki and A. Iiyoshi is appreciated.

References

[1] A. IIYOSHI, et al., in *Plasma Physics and Controlled Nuclear Fusion Research*, London, 1984 (IAEA,Vienna, 1985) Vol.1, p.452

[2] FIDONE,I., GRANATA,G., Nucl. Fusion **11** (1971) 133

[3] ENGELMANN, F., CURATOLO, M., Nucl. Fusion **13** (1973) 497

[4] BOYD, D. A., in Electron Cyclotron Emission and Electron Cyclotron Heating (Proc. 5th Int. Workshop, San Diego, CA, 1985), General Atomics, San Diego, CA (1985) 77

[5] BELL, G. L., et al., Nucl. Fusion **33** (1993) 875

[6] AIROLDI, A, et al., Phys. Fluids **B1** (1989) 2143

[7] OBIKI, T., et al., in *Plasma Physics and Controlled Nuclear Fusion Research*, Washington, DC, 1990 (IAEA, Vienna 1991), Vol.2, p.403

[8] NAGASAKI, K., et al., Fusion Technology **25** (1994) 419

[9] NAGASAKI, K., et al., in Proc. 20th European Conf. Controlled Fusion Plasma Physics, Lisbon, Portugal, 1993 (European Physical Society, 1993) Vol.17C, Pt.I, p.397

[10] BORNATICI, M., et al., Nucl. Fusion **23** (1983) 1153

[11] ZUSHI, H., et al., Nucl. Fusion **28** (1988) 1801

[12] MIZUUCHI, T., et al., J. Nucl. Mater. **176&177** (1990) 1070

[13] HENLE, W., et al., "Study on ECW Transmission Lines for NET/ITER", EUR-FU/80/90-99, Commission of the European Communities (1990)

[14] DOANE, J. L., Int. J. Infrared and Millimeter Waves **13** (1992) 1727

Figure Caption

Fig.1 Schematic view of launched wave. The right and left rotations are defined to be clockwise and counterclockwise, respectively.

Fig.2 Envelope of the square of the electric field for 106.4GHz electron cyclotron wave through the propagation path in the Heliotron-E configuration. The solid and dashed lines denote the cases with and without plasma, respectively. The power is launched from the top of the torus ($z = 0.4m$), and the initial launching condition is $\hat{E}_x = 1, \hat{E}_y = 0$. The axial magnetic field is 1.92T. The plasma profiles are assumed as $n_e(z) = n_e(0)\{1 - (z/a)^6\}, n_e(0) = 1 \times 10^{19} m^{-3}$ $T_e(z) = T_e(0)\{1 - (z/a)^2\}, T_e(0) = 1keV$ and $a = 0.3m$.

Fig.3 Dependence of absorbed power, P_{abs}, on the initial launching conditions, γ and β, (a)left rotation and (b)right rotation. The plasma profiles are the same as in Fig.2. Almost all the power ($\gtrsim$ 99%) is converted into the X-mode and absorbed in the single path when the launched wave has $\gamma = 15°, \beta = -30°$ and right rotation.

Fig.4 Dependence of P_{abs} on central electron density, (a)linear polarization $\gamma = 0°, \beta = 0°$, (b)linear polarization $\gamma = 0°, \beta = 90°$ and (c)elliptic polarization (right rotation) $\gamma = 15°, \beta = -30°$.

Table I Optimization of launching conditions for second harmonic X-mode heating in Heliotron-E, CHS and LHD. Frequencies of ECH are 106.4GHz, 53.2GHz and 84GHz, respectively.

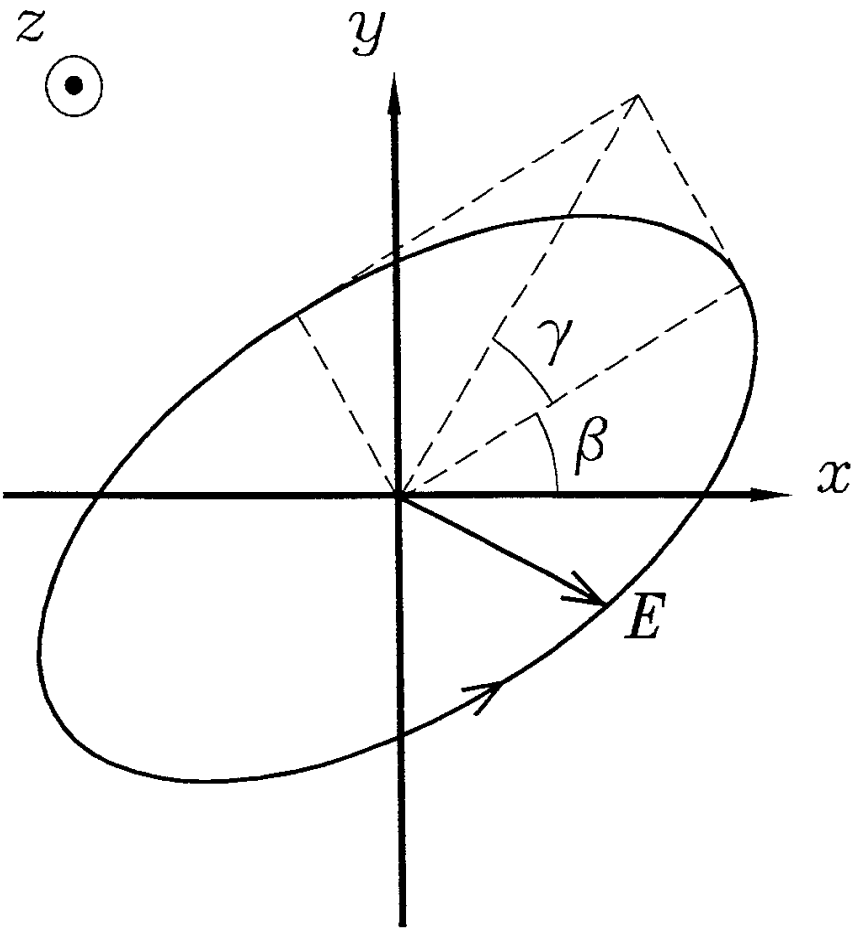

Fig.1

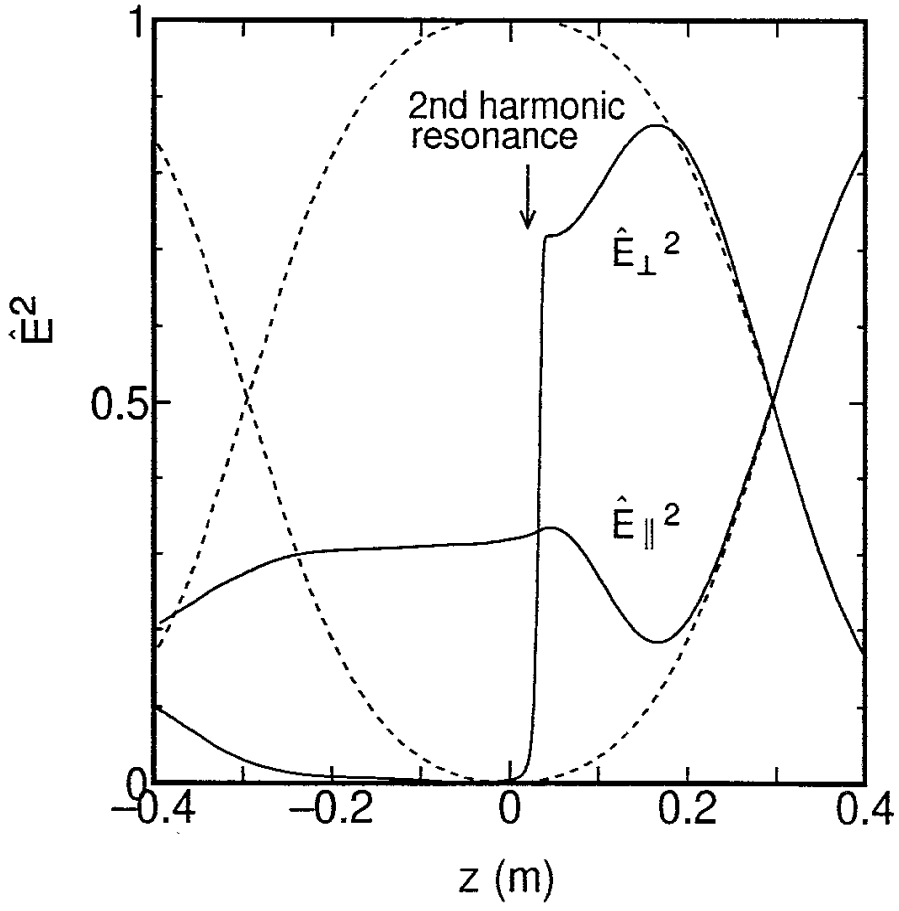
1
0.5
0
$\hat{E}^2$
2nd harmonic
resonance
$\hat{E}_\perp{}^2$
$\hat{E}_\parallel{}^2$
−0.4
−0.2
0
0.2
0.4
z (m)

Fig.2

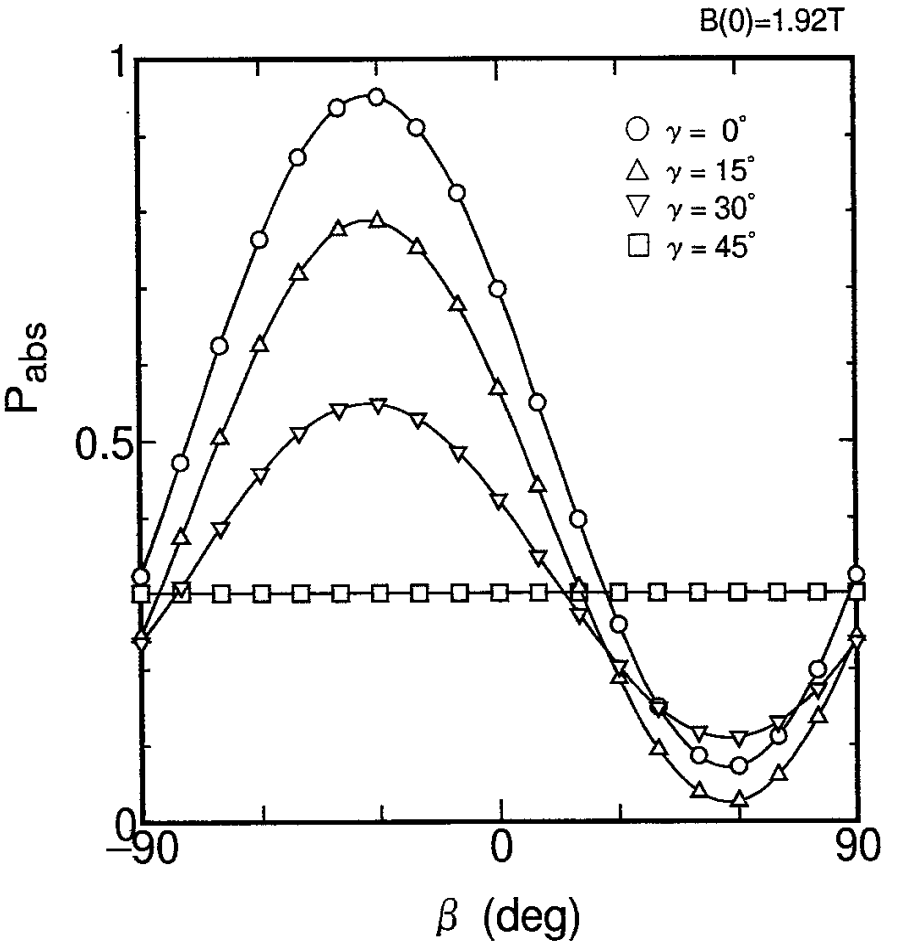
B(0)=1.92T
1
0.5
0
P_{abs}
$\gamma = 0^{\circ}$
$\gamma = 15^{\circ}$
$\gamma = 30^{\circ}$
$\gamma = 45^{\circ}$
−90
0
90
β (deg)

Fig.3(a)

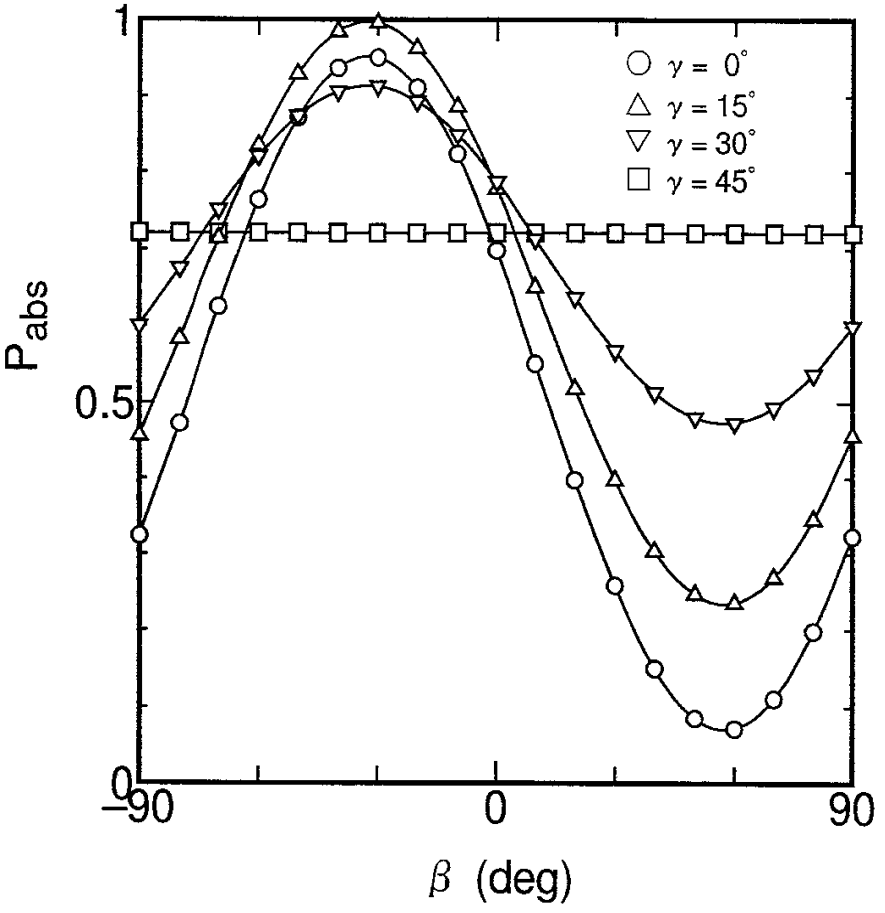

Fig.3 (b)

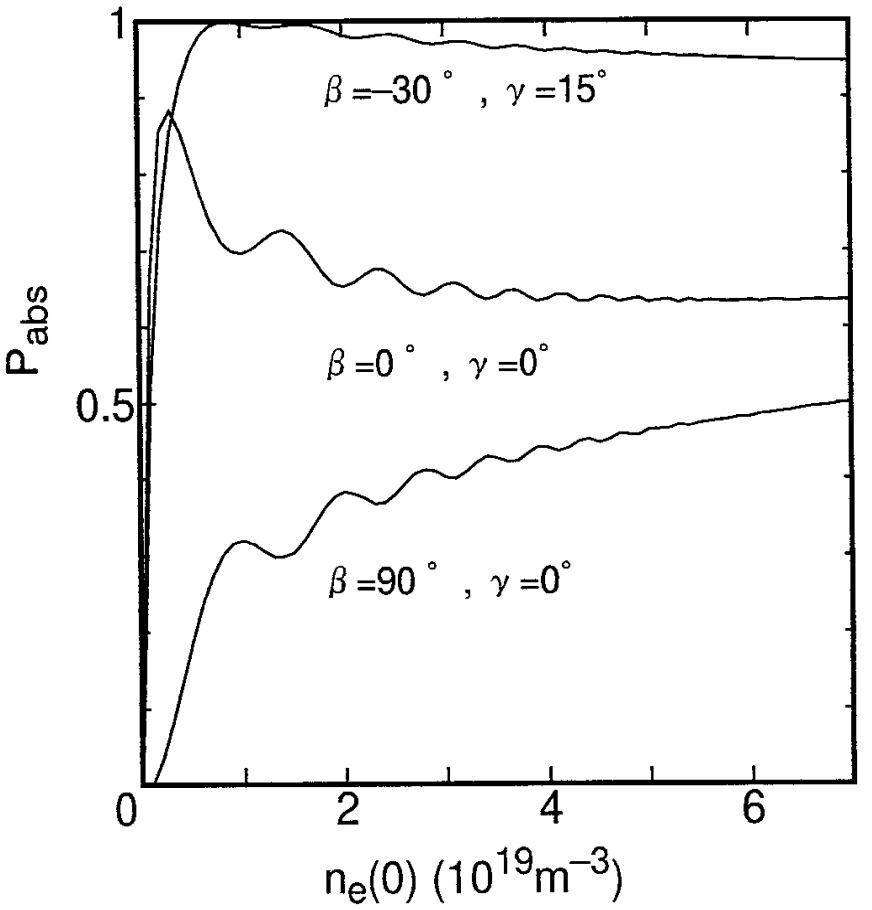
1
0.5
0
P_{abs}
β =–30 ° , γ =15°
β =0 ° , γ =0°
β =90 ° , γ =0°
2
4
6
$n_e(0)$ ($10^{19}m^{-3}$)

Fig.4

Device	β	γ	Rotation
Heliotron–E	$-30°$	$15°$	**Right**
CHS	$30°$	$5°$	**Left**
LHD	$-30°$	$5°$	**Right**

Table I

Recent Issues of NIFS Series

NIFS-290 N. Ohyabu, A. Komori, K. Akaishi, N. Inoue, Y. Kubota, A.I. Livshit, N. Noda, A. Sagara, H. Suzuki, T. Watanabe, O. Motojima, M. Fujiwara, A. Iiyoshi,
Innovative Divertor Concepts for LHD; July 1994

NIFS-291 H. Idei, K. Ida, H. Sanuki, S. Kubo, H. Yamada, H. Iguchi, S. Morita, S. Okamura, R. Akiyama, H. Arimoto, K. Matsuoka, K. Nishimura, K. Ohkubo, C. Takahashi, Y. Takita, K. Toi, K. Tsumori and I. Yamada,
Formation of Positive Radial Electric Field by Electron Cyclotron Heating in Compact Helical System; July 1994

NIFS-292 N. Noda, A. Sagara, H. Yamada, Y. Kubota, N. Inoue, K. Akaishi, O. Motojima, K. Iwamoto, M. Hashiba, I. Fujita, T. Hino, T. Yamashina, K. Okazaki, J. Rice, M. Yamage, H. Toyoda and H. Sugai,
Boronization Study for Application to Large Helical Device; July 1994

NIFS-293 Y. Ueda, T. Tanabe, V. Philipps, L. Könen, A. Pospieszczyk, U. Samm, B. Schweer, B. Unterberg, M. Wada, N. Hawkes and N. Noda,
Effects of Impurities Released from High Z Test Limiter on Plasma Performance in TEXTOR; July. 1994

NIFS-294 K. Akaishi, Y. Kubota, K. Ezaki and O. Motojima,
Experimental Study on Scaling Law of Outgassing Rate with A Pumping Parameter, Aug. 1994

NIFS-295 S. Bazdenkov, T. Sato, R. Horiuchi, K. Watanabe,
Magnetic Mirror Effect as a Trigger of Collisionless Magnetic Reconnection, Aug. 1994

NIFS-296 K. Itoh, M. Yagi, S.-I. Itoh, A. Fukuyama, H. Sanuki, M. Azumi,
Anomalous Transport Theory for Toroidal Helical Plasmas,
Aug. 1994 (IAEA-CN-60/D-III-3)

NIFS-297 J. Yamamoto, O. Motojima, T. Mito, K. Takahata, N. Yanagi, S. Yamada, H. Chikaraishi, S. Imagawa, A. Iwamoto, H. Kaneko, A. Nishimura, S. Satoh, T. Satow, H. Tamura, S. Yamaguchi, K. Yamazaki, M. Fujiwara, A. Iiyoshi and LHD group,
New Evaluation Method of Superconductor Characteristics for Realizing the Large Helical Device; Aug. 1994 (IAEA-CN-60/F-P-3)

NIFS-298 A. Komori, N. Ohyabu, T. Watanabe, H. Suzuki, A. Sagara, N. Noda, K. Akaishi, N. Inoue, Y. Kubota, O Motojima, M. Fujiwara and A. Iiyoshi,
Local Island Divertor Concept for LHD; Aug. 1994 (IAEA-CN-60/F-P-4)

NIFS-299 K. Toi, T. Morisaki, S. Sakakibara, A. Ejiri, H. Yamada, S. Morita, K. Tanaka, N. Nakajima, S. Okamura, H. Iguchi, K. Ida, K. Tsumori,

S. Ohdachi, K. Nishimura, K. Matsuoka, J. Xu, I. Yamada, T. Minami, K. Narihara, R. Akiyama, A. Ando, H. Arimoto, A. Fujisawa, M. Fujiwara, H. Idei, O. Kaneko, K. Kawahata, A. Komori, S. Kubo, R. Kumazawa, T. Ozaki, A. Sagara, C. Takahashi, Y. Takita and T. Watari,
Impact of Rotational-Transform Profile Control on Plasma Confinement and Stability in CHS; Aug. 1994 (IAEA-CN-60/A6/C-P-3)

NIFS-300 H. Sugama and W. Horton,
Dynamical Model of Pressure-Gradient-Driven Turbulence and Shear Flow Generation in L-H Transition; Aug. 1994 (IAEA/CN-60/D-P-I-11)

NIFS-301 Y. Hamada, A. Nishizawa, Y. Kawasumi, K.N. Sato, H. Sakakita, R. Liang, K. Kawahata, A. Ejiri, K. Narihara, K. Sato, T. Seki, K. Toi, K. Itoh, H. Iguchi, A. Fujisawa, K. Adachi, S. Hidekuma, S. Hirokura, K. Ida, M. Kojima, J. Koog, R. Kumazawa, H. Kuramoto, T. Minami, I. Negi, S. Ohdachi, M. Sasao, T. Tsuzuki, J. Xu, I. Yamada, T. Watari,
Study of Turbulence and Plasma Potential in JIPP T-IIU Tokamak;
Aug. 1994 (IAEA/CN-60/A-2-III-5)

NIFS-302 K. Nishimura, R. Kumazawa, T. Mutoh, T. Watari, T. Seki, A. Ando, S. Masuda, F. Shinpo, S. Murakami, S. Okamura, H. Yamada, K. Matsuoka, S. Morita, T. Ozaki, K. Ida, H. Iguchi, I. Yamada, A. Ejiri, H. Idei, S. Muto, K. Tanaka, J. Xu, R. Akiyama, H. Arimoto, M. Isobe, M. Iwase, O. Kaneko, S. Kubo, T. Kawamoto, A. Lazaros, T. Morisaki, S. Sakakibara, Y. Takita, C. Takahashi and K. Tsumori,
ICRF Heating in CHS; Sep. 1994 (IAEA-CN-60/A-6-I-4)

NIFS-303 S. Okamura, K. Matsuoka, K. Nishimura, K. Tsumori, R. Akiyama, S. Sakakibara, H. Yamada, S. Morita, T. Morisaki, N. Nakajima, K. Tanaka, J. Xu, K. Ida, H. Iguchi, A. Lazaros, T. Ozaki, H. Arimoto, A. Ejiri, M. Fujiwara, H. Idei, A. Iiyoshi, O, Kaneko, K. Kawahata, T. Kawamoto, S. Kubo, T. Kuroda, O. Motojima, V.D. Pustovitov, A. Sagara, C. Takahashi, K. Toi and I. Yamada,
High Beta Experiments in CHS; Sep. 1994 (IAEA-CN-60/A-2-IV-3)

NIFS-304 K. Ida, H. Idei, H. Sanuki, K. Itoh, J. Xu, S. Hidekuma, K. Kondo, A. Sahara, H. Zushi, S.-I. Itoh, A. Fukuyama, K. Adati, R. Akiyama, S. Bessho, A. Ejiri, A. Fujisawa, M. Fujiwara, Y. Hamada, S. Hirokura, H. Iguchi, O. Kaneko, K. Kawahata, Y. Kawasumi, M. Kojima, S. Kubo, H. Kuramoto, A. Lazaros, R. Liang, K. Matsuoka, T. Minami, T. Mizuuchi, T. Morisaki, S. Morita, K. Nagasaki, K. Narihara, K. Nishimura, A. Nishizawa, T. Obiki, H. Okada, S. Okamura, T. Ozaki, S. Sakakibara, H. Sakakita, A. Sagara, F. Sano, M. Sasao, K. Sato, K.N. Sato, T. Saeki, S. Sudo, C. Takahashi, K. Tanaka, K. Tsumori, H.Yamada, I. Yamada, Y. Takita, T. Tuzuki, K. Toi and T. Watari,
Control of Radial Electric Field in Torus Plasma; Sep. 1994
(IAEA-CN-60/A-2-IV-2)

NIFS-305 T. Hayashi, T. Sato, N. Nakajima, K. Ichiguchi, P. Merkel, J. Nührenberg, U. Schwenn, H. Gardner, A. Bhattacharjee and

C.C.Hegna,
Behavior of Magnetic Islands in 3D MHD Equilibria of Helical Devices;
Sep. 1994 (IAEA-CN-60/D-2-II-4)

NIFS-306 S. Murakami, M. Okamoto, N. Nakajima, K.Y. Watanabe, T. Watari, T. Mutoh, R. Kumazawa and T. Seki,
Monte Carlo Simulation for ICRF Heating in Heliotron/Torsatrons;
Sep. 1994 (IAEA-CN-60/D-P-I-14)

NIFS-307 Y. Takeiri, A. Ando, O. Kaneko, Y. Oka, K. Tsumori, R. Akiyama, E. Asano, T. Kawamoto, T. Kuroda, M. Tanaka and H. Kawakami,
Development of an Intense Negative Hydrogen Ion Source with a Wide-Range of External Magnetic Filter Field; Sep. 1994

NIFS-308 T. Hayashi, T. Sato, H.J. Gardner and J.D. Meiss,
Evolution of Magnetic Islands in a Heliac; Sep. 1994

NIFS-309 H. Amo, T. Sato and A. Kageyama,
Intermittent Energy Bursts and Recurrent Topological Change of a Twisting Magnetic Flux Tube; Sep.1994

NIFS-310 T. Yamagishi and H. Sanuki,
Effect of Anomalous Plasma Transport on Radial Electric Field in Torsatron/Heliotron; Sep. 1994

NIFS-311 K. Watanabe, T. Sato and Y. Nakayama,
Current-profile Flattening and Hot Core Shift due to the Nonlinear Development of Resistive Kink Mode; Oct. 1994

NIFS-312 M. Salimullah, B. Dasgupta, K. Watanabe and T. Sato,
Modification and Damping of Alfvén Waves in a Magnetized Dusty Plasma; Oct. 1994

NIFS-313 K. Ida, Y. Miura, S -I. Itoh, J.V. Hofmann, A. Fukuyama, S. Hidekuma, H. Sanuki, H. Idei, H. Yamada, H. Iguchi, K. Itoh,
Physical Mechanism Determining the Radial Electric Field and its Radial Structure in a Toroidal Plasma; Oct. 1994

NIFS-314 Shao-ping Zhu, R. Horiuchi, T. Sato and The Complexity Simulation Group,
Non-Taylor Magnetohydrodynamic Self-Organization; Oct. 1994

NIFS-315 M. Tanaka,
Collisionless Magnetic Reconnection Associated with Coalescence of Flux Bundles; Nov. 1994

NIFS-316 M. Tanaka,
Macro-EM Particle Simulation Method and A Study of Collisionless Magnetic Reconnection; Nov. 1994

NIFS-317 A. Fujisawa, H. Iguchi, M. Sasao and Y. Hamada,
Second Order Focusing Property of 210° Cylindrical Energy Analyzer; Nov. 1994

NIFS-318 T. Sato and Complexity Simulation Group,
Complexity in Plasma - A Grand View of Self- Organization; Nov. 1994

NIFS-319 Y. Todo, T. Sato, K. Watanabe, T.H. Watanabe and R. Horiuchi,
MHD-Vlasov Simulation of the Toroidal Alfvén Eigenmode; Nov. 1994

NIFS-320 A. Kageyama, T. Sato and The Complexity Simulation Group,
Computer Simulation of a Magnetohydrodynamic Dynamo II: Nov. 1994

NIFS-321 A. Bhattacharjee, T. Hayashi, C.C.Hegna, N. Nakajima and T. Sato,
Theory of Pressure-induced Islands and Self-healing in Three-dimensional Toroidal Magnetohydrodynamic Equilibria; Nov. 1994

NIFS-322 A. Iiyoshi, K. Yamazaki and the LHD Group,
Recent Studies of the Large Helical Device; Nov. 1994

NIFS-323 A. Iiyoshi and K. Yamazaki,
The Next Large Helical Devices; Nov. 1994

NIFS-324 V.D. Pustovitov
Quasisymmetry Equations for Conventional Stellarators; Nov. 1994

NIFS-325 A. Taniike, M. Sasao, Y. Hamada, J. Fujita, M. Wada,
The Energy Broadening Resulting from Electron Stripping Process of a Low Energy Au^- Beam; Dec. 1994

NIFS-326 I. Viniar and S. Sudo,
New Pellet Production and Acceleration Technologies for High Speed Pellet Injection System "HIPEL" in Large Helical Device; Dec. 1994

NIFS-327 Y. Hamada, A. Nishizawa, Y. Kawasumi, K. Kawahata, K. Itoh, A. Ejiri, K. Toi, K. Narihara, K. Sato, T. Seki, H. Iguchi, A. Fujisawa, K. Adachi, S. Hidekuma, S. Hirokura, K. Ida, M. Kojima, J. Koong, R. Kumazawa, H. Kuramoto, R. Liang, T. Minami, H. Sakakita, M. Sasao, K.N. Sato, T. Tsuzuki, J. Xu, I. Yamada, T. Watari,
Fast Potential Change in Sawteeth in JIPP T-IIU Tokamak Plasmas; Dec. 1994

NIFS-328 V.D. Pustovitov,
Effect of Satellite Helical Harmonics on the Stellarator Configuration; Dec. 1994

NIFS-329 K. Itoh, S-I. Itoh and A. Fukuyama,
A Model of Sawtooth Based on the Transport Catastrophe; Dec. 1994